

Output Current Control via Primary Side Controller using Wireless Communication for WPT System

Suttisak Uraiwong¹, Phongthanaphat Lamunphak¹, Athit Suanchuto¹, Hatta Sawachan¹ and Kan Voottipruex^{1*}

¹Department of Electrical Engineering Technology, College of Industrial Technology, King Mongkut's University of Technology North Bangkok, Bangkok, Thailand, hatta.s@cit.kmutnb.ac.th kan.v@cit.kmutnb.ac.th*

Abstract

Variations in the output parameters of a Wireless Transfer (WPT) system are unavoidable, particularly due to load fluctuations caused by the battery's state of charge (SOC). Therefore, an appropriate compensation circuit topology is essential for maintaining either a constant output voltage (CV) or a constant output current (CC). This paper proposes an output current control method for a WPT system using a primary-side controller combined with wireless communication. A Series-Series (SS) compensation topology is adopted to ensure a load-independent output current characteristic. NodeMCUs are employed on both the primary and secondary sides to enable real-time feedback and control. Experimental results demonstrate a stable output current of 2 A across load resistances ranging from 6 to 20 Ω , with a maximum power transfer efficiency of 87.163% achieved at a 16 Ω load.

Keywords: Output current control, Wireless communication, Wireless power transfer.

1. General Information

A Wireless Power Transfer (WPT) system transfers power to a load via a loosely coupled transformer without physical contact. This technology can be found in diverse areas such as electric vehicles (EVs) [1], autonomous robotics [2], and consumer electronics [3]. Compensation circuit topologies are commonly applied in Inductive Power Transfer (IPT) or Wireless Power Transfer (WPT) systems. These circuits are tuned to resonate with the coil inductances to maximize power transfer capability on both sides, enhance system efficiency by enabling softswitching techniques such as Zero Voltage Switching (ZVS) for the primary-side inverter, and achieve the desired output characteristics. The output voltage or current of WPT systems can vary across a wide range of equivalent load conditions. Therefore, a suitable compensation circuit topology is essential for maintaining either a constant output voltage (CV) or constant output current (CC), independent of the load conditions. Conventional compensation topologies include four topologies, each with a single compensation element on both the primary and secondary sides: Series-Series (SS), Series-Parallel (SP), Parallel-Series (PS), and Parallel-Parallel (PP) [4]. A comparison of these four basic topologies is presented in Table 1.

A primary-side parallel compensation circuit is typically used with a current source inverter (CSI), but it results in a larger hardware size due to the required DC- Table 1 Comparison of four basic topologies

Tuble 1 Comparison of four busic topologies				
Topo- logy	Primary capacitance	Operating frequency	Output	
SS	$C_p = \frac{1}{\omega_0^2 L_p}$	Independent of <i>M</i> and <i>R</i>	CC	
SP	$C_p = \frac{1}{\omega_0^2 \left(L_p - \frac{M^2}{L_s} \right)}$	Depends on M	CV	
PS	$C_{p} = \frac{L_{p}}{\left(\frac{\omega_{0}^{2}M^{2}}{R}\right)^{2} + \omega_{0}^{2}L_{p}^{2}}$	Depends on <i>M</i> and <i>R</i>	CC	
PP	$C_{p} = \frac{L_{p} - \frac{M^{2}}{L_{s}}}{\left(\frac{M^{2}R}{L_{s}^{2}}\right)^{2} + \omega_{0}^{2} \left(L_{p} - \frac{M^{2}}{L_{s}}\right)^{2}}$	Depends on <i>M</i> and <i>R</i>	CV	

link inductor. Topologies with a parallel-compensated primary, such as Parallel-Series (PS) and Parallel-Parallel (PP), provide constant output current (CC) and constant output voltage (CV), respectively, under resonant conditions. However, the resonant or operating frequency in these configurations depends on the mutual inductance and load resistance. As a result, the operating frequency must be tracked, or the primary-side capacitance must be tuned to accommodate specific variations.

other hand, a primary-side series compensation circuit is commonly used with a voltage source inverter (VSI), enabling a more compact hardware design. The Series-Parallel (SP) topology provides a constant output voltage (CV), but its operating frequency still depends on the mutual inductance. Therefore, similar to PS and PP topologies, the operating frequency must be tracked, or the primary-side capacitance in the SP topology must be adjusted to account for variations. The Series-Series (SS) topology is extensively studied and widely implemented. One of its key advantages is that the resonant frequency remains independent of variations in both the load and the mutual inductance between the primary and secondary coils. As a result, the impedance reflected from the secondary to the primary side is purely resistive. This characteristic significantly simplifies the control strategy, allowing fixed frequency operation. Moreover, the SS topology inherently exhibits a constant output current or load-independent output current characteristic, which is highly beneficial for battery วันที่ 19-21 พฤศจิกายน 2568 ณ โรงแรมฟูราม่า จังหวัดเชียงใหม่



charging applications during the constant current (CC) mode [5]. However, regulating a constant charging current under varying system parameters such as load fluctuations or air gap changes remains critical. To address this, conventional systems often incorporate converters on the secondary side to precisely regulate the charging current. Nevertheless, this approach results in a more complex and bulky secondary side structure, with an increased number of components, greater complexity, and larger overall system size [6].

This paper presents output current control through a primary side controller using wireless communication for the proposed WPT system. The control system is specifically designed to provide accurate current regulation using NodeMCUs. The paper is organized as follows: Section 2 presents an analysis of the design parameters for the SS topology, Section 3 describes the proposed WPT system, and Section 4 provides experimental results to confirm the system performance.

Analysis of Series-Series Topology

An SS topology consists of a primary coil (L_p) and a secondary coil (L_s) magnetically coupled through a mutual inductance (M). The coupling coefficient can be expressed as

$$k = \frac{M}{\sqrt{L_p L_s}} \tag{1}$$

To compensate the inductive reactance of the coils and achieve resonance, a capacitor is placed in series with each coil, C_p on the primary side and C_s on the secondary side. The circuit is driven by a high-frequency AC voltage source (V_p) on the primary side, and the transferred power is delivered to a load (R_L) on the secondary side as shown in Figure 1. The secondary impedance can be calculated

$$Z_s = j\omega L_s + \frac{1}{j\omega C_s} + R_L \tag{2}$$

The reflected impedance can be expressed by

$$Z_r = \frac{\omega^2 M^2}{Z_-} \tag{3}$$

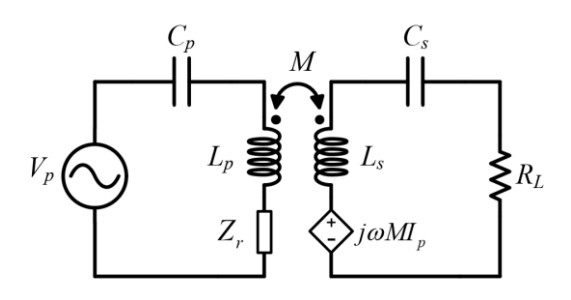


Fig. 1 Equivalent of SS topology

Hence, the input impedance (Z_{in}) can be described by

$$Z_{in} = j\omega L_p + \frac{1}{j\omega C_p} + Z_r \tag{4}$$

The primary and secondary circuits are tuned to resonate at the same angular frequency (ω_{θ}) . This resonant condition is crucial for maximizing power transfer efficiency. The resonant frequency is determined by the inductance and capacitance values in each circuit, which expressed by

$$\omega_0 = \frac{1}{\sqrt{L_p C_p}} = \frac{1}{\sqrt{L_s C_s}} \tag{5}$$

The SS topology exhibits a load-independent output current characteristic at the resonant frequency (ω_{θ}) . The secondary current (I_s) can be expressed as

$$I_s(\omega_0) = j \frac{V_p}{\omega_0 M} \tag{6}$$

Therefore, the output current (I_o) can be calculated by

$$I_o = \left(\frac{2\sqrt{2}}{\pi}\right) I_s\left(\omega_0\right) \tag{7}$$

3. Proposed WPT System

A circular coil was chosen to validate the proposed WPT system. The coil dimensions, designed to suit lowpower applications with a vertical air gap of 5 cm, are shown in Figure 2.

Table 2 Electrical parameters for the proposed WPT system

Parameters	Values	Unit	
Inverter frequency (f_{inv})	85	kHz	
Buck converter frequency (f_{buck})	25	kHz	
Input voltage (V_{IN})	48	V	
Primary coil inductance (L_p)	74	μΗ	
Secondary coil inductance (L_s)	74	μΗ	
Primary capacitance (C_p)	47	nF	
Secondary capacitance (C_s)	47	nF	
Mutual inductance (M)	19.24	μΗ	



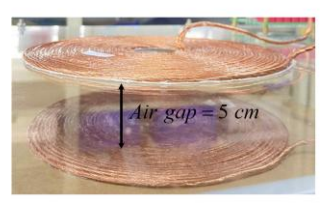


Fig. 2 Coil dimensions and vertical air gap arrangement



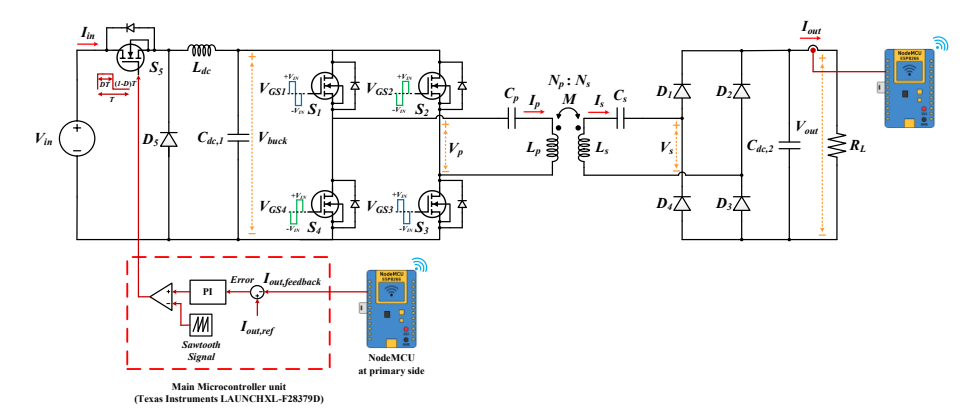


Fig. 3 Proposed WPT system

The proposed WPT system comprises a primary and a secondary circuit. The primary circuit integrates a buck converter, a full-bridge inverter, a primary capacitor, and a primary coil. The secondary circuit contains a secondary coil, a capacitor, a bridge rectifier, and a capacitive filter connected to a load. Figure 3 provides a schematic illustration of the system, and its specified electrical parameters are presented in Table 2. An input voltage of 48 volts is supplied to a buck converter, which operates at a switching frequency of 25 kHz. The amplitude of the primary voltage is regulated by a PI controller. This controller continuously adjusts the buck converter's output by comparing a reference current to feedback output current data sent wirelessly from the secondary side via NodeMCUs. The inverter then converts the regulated DC voltage into a high-frequency square-wave voltage, operating at a fixed resonant frequency (f_0) of 85 kHz.

4. Experiment

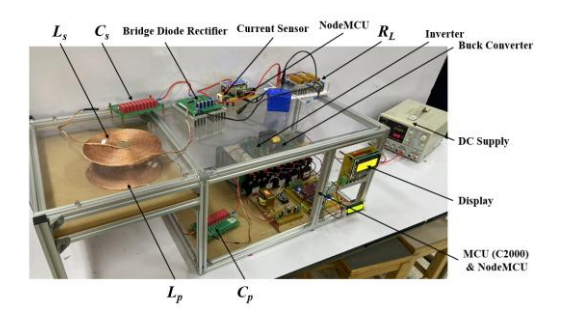


Fig. 4 Hardware prototype

The hardware prototype was constructed to verify the proposed method using a 6 Ω load, as shown in Figure 4. The experimental results in Figure 5 show that the DC input voltage (V_{in}) was 47.9 V, with an input current (I_{in}) of 612 mA. Correspondingly, the experimental results in Figure 6 illustrate that the primary voltage (V_p) was 26.39 V, with an primary current (I_p) of 1.41 A, while the secondary voltage (V_s) was 14.02 V with an secondary current (I_s) of 2.23 A as shown in Figure 7.

Correspondingly, the experimental results in Figure 8 illustrate that the output voltage (V_{out}) was 11.54 V, with an output current (I_{out}) of 2.03 A.

Furthermore, the graph in Figure 9 shows the relationship between load resistance and the output parameters (V_{out} and I_{out}) of the proposed WPT system. The output current (I_{out}) remains nearly constant at approximately 2 A over the tested load range of 6 Ω to 20 Ω , indicating effective load-independent characteristics. Meanwhile, the output voltage (V_{out}) increases linearly from about 11.5 V to over 38.99 V as the load resistance increases.

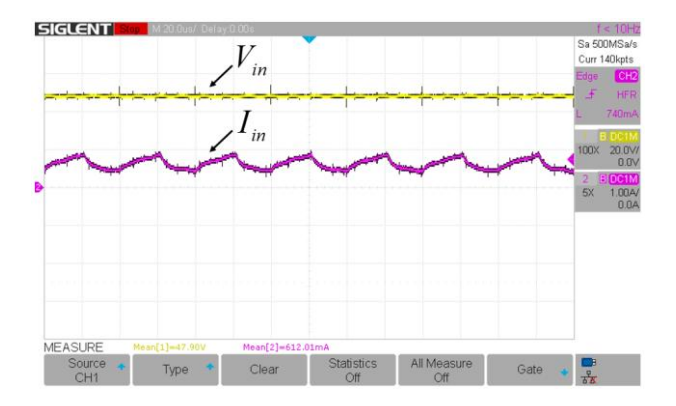


Fig. 5 Experimental waveforms of V_{in} and I_{in}

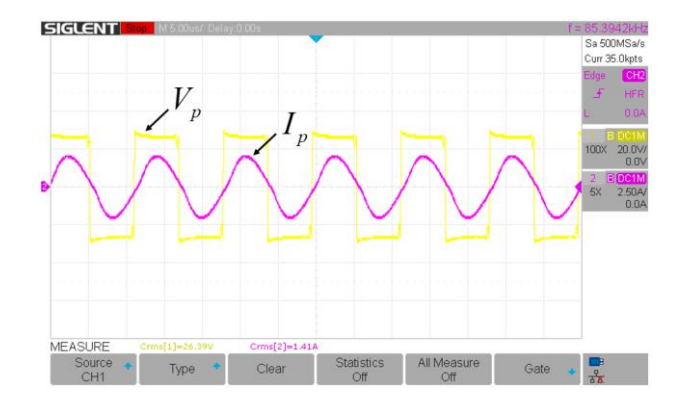


Fig. 6 Experimental waveforms of V_p and I_p



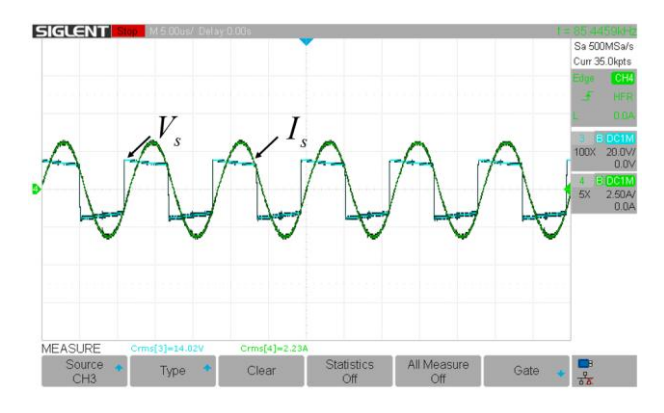


Fig. 7 Experimental waveforms of V_s and I_s

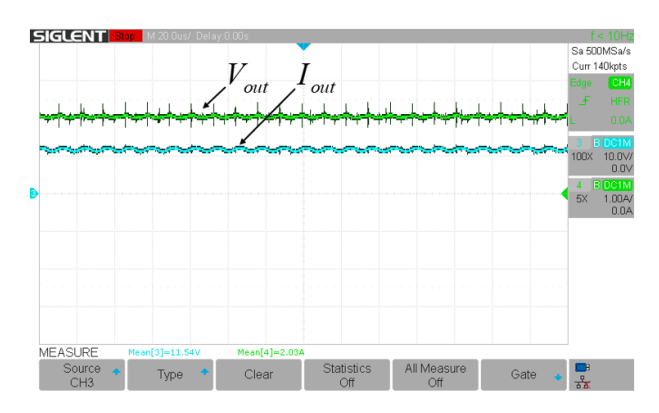


Fig. 8 Experimental waveforms of V_{out} and I_{out}

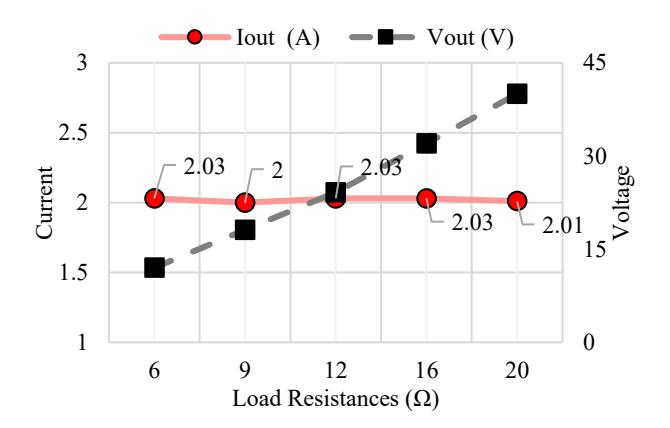


Fig. 9 V_{out} and I_{out} versus different load resistances

The efficiency shown in Figure 10 initially increases from 79.912% at a load of 6 Ω , reaching a maximum value of 87.163% at 16 Ω . Beyond this load resistance value, efficiency gradually decreases, falling to 84.424% at a load of 20 Ω . These results indicate that the system operates most efficiently at a load of 16 Ω .

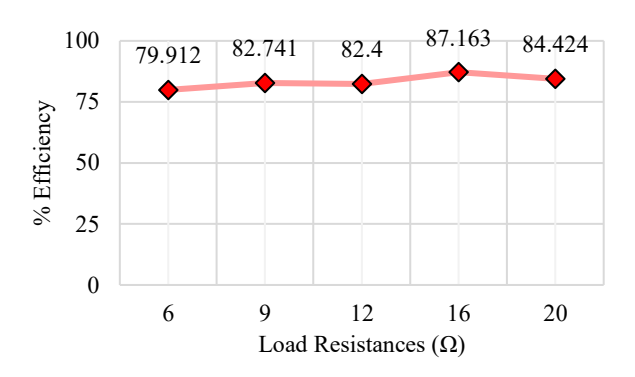


Fig. 10 Efficiency versus different load resistances

5. Conclusions

The proposed SS WPT system effectively maintains load-independent output current control using primary-side regulation and wireless feedback. Experimental validation demonstrates that the system maintains a constant output current of approximately 2 A over varying load conditions (6 Ω to 20 Ω), while achieving a peak efficiency of 87.163% at a 16 Ω load. These results highlight the effectiveness of the primary-side control strategy in WPT applications.

References

- [1] D. Patil, M. K. Mcdonough, J. M. Miller, B. Fahimi, and P. T. Balsara, "Wireless power transfer for vehicular applications: Overview and challenges," *IEEE Trans. Transp. Electrific.*, vol. 4, no. 1, pp. 3–37, Mar. 2018.
- [2] C. Zhu, J. Yu, Y. Gu, J. Gao, H. Yang, R. Mai, Y. Li, and Z. He, "Analysis and design of cost-effective WPT systems with dual independently regulatable outputs for automatic guided vehicles," *IEEE Trans. Power Electron.*, vol. 36, no. 6, pp. 6183–6193, Jun. 2021.
- [3] J. Park, D. Kim, K. Hwang, H. H. Park, S. I. Kwak, J. H. Kwon, and S. Ahn, "A resonant reactive shielding for planar wireless power transfer system in smartphone application," *IEEE Trans. Electromagn. Compat.*, vol. 59, no. 2, pp. 695–703, Apr. 2017.
- [4] V. Shevchenko, O. Husev, R. Strzelecki, B. Pakhaliuk, N. Poliakow, and N. Strzelecka, "Compensation topologies in IPT systems: Standards, requirements, classification, analysis, comparison and application," *IEEE Access*, vol. 7, pp. 120559–120580, 2019.
- [5] W. Zhang, S.-C. Wong, C. K. Tse, and Q. Chen, "Load-independent duality of current and voltage outputs of a series- or parallel-compensated inductive power transfer converter with optimized efficiency," *IEEE J. Emerg. Sel. Topics Power Electron.*, vol. 3, no. 1, pp. 137–146, Mar. 2015.
- [6] T. Diekhans and R. W. De Doncker, "A dual-side controlled inductive power transfer system optimized for large coupling factor variations and partial load,"

The 48th Electrical Engineering Conference (EECON-48)

วันที่ 19-21 พฤศจิกายน 2568 ณ โรงแรมฟูราม่า จังหวัดเชียงใหม่

IEEE Trans. Power Electron., vol. 30, no. 11, pp. 6320–6328, Nov. 2015.



Suttisak Uraiwong : received a vocational certificate in Electrical Power from Saraburi Technical College in 2021 and an advanced vocational certificate in Power Transmission Technology from Saraburi Technical College in 2023. He is

currently studying for a Bachelor of Industrial Technology in Electrical and Power Electronics Technology, Department of Electrical Engineering Technology, College of Industrial Technology, King Mongkut's University of Technology North Bangkok (KMUTNB).



Phongthanaphat Lamunphak: received a vocational certificate in Electrical Power from Saraburi Technical College in 2021 and an advanced vocational certificate in Power Transmission Technology from Saraburi

Technical College in 2023. He is currently studying for a Bachelor of Industrial Technology in Electrical and Power Electronics Technology, Department of Electrical Engineering Technology, College of Industrial Technology, King Mongkut's University of Technology North Bangkok (KMUTNB).



Athit Suanchuto: received a vocational certificate in Automotive from Ratchaburi Technical College in 2021 and an advanced vocational certificate in Electrical Power from Ratchaburi Technical College in 2023. He is currently

studying for a Bachelor of Industrial Technology in Electrical and Power Electronics Technology, Department of Electrical Engineering Technology, College of Industrial Technology, King Mongkut's University of Technology North Bangkok (KMUTNB).



Hatta Sawachan: received the B.Ind.Tech. degree in Power Electronics Technology from King Mongkut's University of Technology North Bangkok (KMUTNB), Bangkok, Thailand, in 2014, and the M.Eng. degree in Electrical

Engineering (Automatic Control) from the same university in 2017. He is currently an Assistant Professor with the Department of Electrical Engineering Technology, College of Industrial Technology, KMUTNB. His research interests include Power Electronics (Power Converter, Grid Connection, Electric Drive), Control System, and Digital Control.





Kan Voottipruex: received the B.Eng. degree in Electronic and Telecommunication Engineering from King Mongkut's University of Technology Thonburi (KMUTT), Bangkok, in 2014, and the M.Eng. degree

in Electrical Engineering from King Mongkut's University of Technology Thonburi (KMUTT), Bangkok, in 2017. He is currently a lecturer with the Department of Electrical Engineering Technology, College of Industrial Technology, King Mongkut's University of Technology North Bangkok (KMUTNB). His research interests include inductive power transfer systems (IPT), wireless charging applications, and renewable energy applications.